Acta Cryst. (1995). B51, 758–767

Structures Containing Shift-Lattice Distributed Planar Faults

BY R. J. D. TILLEY* AND R. P. WILLIAMS

School of Engineering and Department of Physics and Astronomy, University of Wales College of Cardiff, PO Box 925, Cardiff CF2 1YF, Wales

(*Received* 12 *December* 1993; *accepted* 2 *April* 1995)

Abstract

Structures which can be considered to be built up from slabs of identical material, each displayed by a constant amount with respect to its neighbours, are described in terms of the shift lattice and the general form of their diffraction patterns has been derived. The theory is illustrated by reference to the $(M,\mathrm{Ti})O_{2-x}$ crystallographic shear (CS) structures, the alloy Au_5Mn_2 antiphase domain structure and a number of hypothetical constructions.

1. Introduction

As the techniques of recording and interpreting diffraction patterns have improved, the description of non-stoichiometric and other similarly complex phases has evolved from that of an average structure towards more sophisticated models. One of the more fruitful of these developements is the recognition that many of these compounds are built up from a stacking of identical slabs of a parent structure (Wadsley, 1963; Hyde & Andersson, 1989; Tilley, 1987). It is often convenient to focus attention upon the boundaries between these slabs of perfect structure. In the case where the slab thicknesses are regular, the boundaries are ordered. Changes in the thickness of the ordered slabs produces a homologous series of stoichiometric compounds characterized by wider or narrower boundary spacings. In the cases where the slabs are of variable thickness, the boundaries can be thought of as disordered planar defects in a host matrix. Variable numbers of such defects yield a disordered phase which will frequently be operationally non-stoichiometric. One of the best known examples of this structural principle is to be found in the crystallographic shear (CS) phases (Hyde & Andersson, 1989, pp. 27 and 98; Harburn, Parry, Tilley & Williams, 1992).

In a previous publication it was noted that these phases could be treated in terms of the *shift lattice*, an alternative concept in which attention is focused upon the slabs of structure rather than the boundaries (Harburn, Tilley, Williams & Williams, 1991, 1993; Tilley & Williams, 1995). The elaboration of this idea is presented in this paper. The theory of the shift lattice for general planar boundaries, which has not been developed previously, is presented in the following section. The application of the theory to an analysis of diffraction patterns is outlined by way of two apparently quite different examples, the TiO_{2-x} system which contains CS planes and the $Au_{3-x}Mn$ system in which antiphase boundaries are found. Finally, the way in which the shift lattice, with appropriate parameters, can be used to construct various new structures and the diffraction patterns which such structures would produce concludes the paper.

2. Shift-lattice distributed planar faults

2.1. *Preliminary remarks*

The structures under consideration in this paper are essentially three-dimensional. For simplicity, however, the exposition will be two-dimensional, there being generally no formal difficulty in the extension to three dimensions. The mathematical entity at the heart of the discussions is the two- (or three-) dimensional comb and we therefore start with some background information concerning it. It consists of a two-dimensional lattice of unit-magnitude point-delta functions, that is to say that there is a delta function with a point singularity at every lattice point on the plane. If a single such delta function with its singularity at the origin of $\mathbf{r}$ space ($\mathbf{r}$ being the position vector on the plane) is given the symbol $\delta(\mathbf{r})$, then the comb may be described by

$$\sum_m \sum_n \delta\{\mathbf{r} - (m\boldsymbol{a}_1 + n\boldsymbol{a}_2)\},$$

where $\boldsymbol{a}_1$ and $\boldsymbol{a}_2$ are the lattice parameters and the summations (as are all summations in this paper) are between $-\infty$ and $+\infty$. Hsu (1967) has provided a useful notation for the one-dimensional comb; we extend this to two dimensions and define the two-dimension comb as

$$\delta_{\boldsymbol{a}_1,\boldsymbol{a}_2}(\mathbf{r}) = \sum_m \sum_n \delta[\mathbf{r} - (m\boldsymbol{a}_1 + n\boldsymbol{a}_2)]. \qquad (2.1)$$

The notation on the left-hand side of (2.1) immediately displays the space ($\mathbf{r}$) in which the comb and also the lattice parameters $\boldsymbol{a}_1$ and $\boldsymbol{a}_2$ in this space exist. Its great advantage in analytical work is that it 'hides' the double summation on the right-hand side of (2.1), the summation often not being explicitly needed. The extension of

* Author to whom correspondence should be addressed.

Hsu's notation to three dimensions is obvious. We finally remark, concerning (2.1), that we have found it slightly advantageous to use Greek letters to symbolize distances, allowing the use of Roman letters for other purposes, particularly when comparing parameters in our work with those used by other workers in the field.

2.2. *Planar fault structures*

Fig. 1 illustrates schematically a two-dimensional example of the structures under consideration in this paper. Each circle represents the singularity of a point-delta function and we see at once that the structure has lattice-like attributes. Closer examination of the figure reveals that the region between the dotted lines AA' and BB' is a 'slab' of perfect crystal lattice, as is the region between the lines CC' and DD'. (The dotted lines are assumed to be infinitely long.) However, between the two regions, there is a fault in that the lattice of the second region is displaced with respect to that in the first region by a vector displacement γ. (It may here be remarked that there is an infinite number of ways of defining γ, namely the vector distance from any delta-function singularity in the first region to any singularity in the second. No essential difference in the analysis, however, ensues upon the particular definition of γ and, in practice, we choose the most convenient. More will be said of γ later.)

Consider now the central slab (*i.e.* that between AA' and BB') in Fig. 1. If we let g be a function of r (r having the rectangular Cartesian coordinates x and y illustrated), which is unity between AA' and BB' and zero elsewhere, then the set of delta functions whose singularities lie between these two dotted lines can be represented by the product of g and $\delta_{\mathbf{a}_1,\mathbf{a}_2}(\mathbf{r})$. We concentrate further on the nature of g. It is clear from Fig. 1 that if the dotted lines were vertical, then g would be a function of x only and would be constant along any line parallel to the y axis. Indeed, with rect(x) defined in the usual way [*i.e.* rect(x) = 1 for $-\frac{1}{2} < x < +\frac{1}{2}$ and zero elsewhere], then for vertical dotted lines and a slab of width w_1, we would have $g = \text{rect}(x/w_1) = \text{rect}(w_1^* x) = \text{rect}(w_1^* \mathbf{i} \cdot \mathbf{r})$, where $w_1^* = 1/w_1$. The generalization of this for an arbitrary angle of dotted lines is

$$g = \text{rect}(\mathbf{w}_1^* \cdot \mathbf{r}),$$

where the mutually perpendicular set of vectors $\mathbf{w}_1, \mathbf{w}_2$ has $\mathbf{w}_1^*, \mathbf{w}_2^*$ as its consequently mutually perpendicular set of reciprocal vectors. The modulus of the vector $\mathbf{w}_1^*$ is thus the reciprocal of that of $\mathbf{w}_1$. The vector $\mathbf{w}_2$ (perpendicular to $\mathbf{w}_1$) may, however, be of any finite length and has no real physical significance; it is defined merely to provide a pair of vectors (namely $\mathbf{w}_1$ and $\mathbf{w}_2$) to enable us to assign meaning to $\mathbf{w}_1^*$.

The Fourier-transform derivation in §5 does not depend upon the fact that the g function is a rect function; we will therefore leave it arbitrary at $g(\mathbf{w}_1^* \cdot \mathbf{r})$ and note therefore that the central slab may be mathematically represented as $g(\mathbf{w}_1^* \cdot r)\delta_{\mathbf{a}_1,\mathbf{a}_2}(\mathbf{r})$. The slab to the right of the central one has its g function displaced by a vector distance $\boldsymbol{\beta}$ (which may be taken as parallel to $\mathbf{w}_1^*$, although this is not essential), whose function is now therefore $g\{\mathbf{w}_1^* \cdot (\mathbf{r} - \boldsymbol{\beta})\}$ and has its lattice displaced by γ so that the comb appropriate to it is

$$\delta_{\mathbf{a}_1,\mathbf{a}_2}(\mathbf{r} - \gamma).$$

This slab is therefore represented by

$$g[\mathbf{w}_1^* \cdot (\mathbf{r} - \boldsymbol{\beta})]\delta_{\mathbf{a}_1,\mathbf{a}_2}(\mathbf{r} - \gamma).$$

In general, the mth slab to the right of the central one is therefore represented by

$$g[\mathbf{w}_1^* \cdot (\mathbf{r} - m\boldsymbol{\beta})]\delta_{\mathbf{a}_1,\mathbf{a}_2}(\mathbf{r} - m\gamma),$$

and so the entire structure, $f(\mathbf{r})$, is represented by

$$f(\mathbf{r}) = \sum_m g[\mathbf{w}_1^* \cdot (\mathbf{r} - m\boldsymbol{\beta})]\delta_{\mathbf{a}_1,\mathbf{a}_2}(\mathbf{r} - m\gamma). \qquad (2.2)$$

In three dimensions, we replace the $\delta_{\mathbf{a}_1,\mathbf{a}_2}$ in (2.2) by $\delta_{\mathbf{a}_1,\mathbf{a}_2,\mathbf{a}_3}$ and note that the vector $\boldsymbol{\beta}$, which defines the interslab distance, is not necessarily in the $\mathbf{a}_1$, $\mathbf{a}_2$ plane. In general, therefore, these planes are in an arbitrary direction with respect to the underlying sublattice vectors.

We now examine γ in more detail. It proves useful to express it as a linear combination of $\mathbf{a}_1$ and $\mathbf{a}_2$, thus

$$\gamma = \varepsilon_1 \mathbf{a}_1 + \varepsilon_2 \mathbf{a}_2. \qquad (2.3)$$

Here, the εs are dimensionless quantities which are most conveniently taken as positive proper fractions. Examination of the example in Fig. 1 reveals that ε_1 – the fraction of $\mathbf{a}_1$ in its direction by which the lattice has been displaced across the fault – is $\frac{1}{4}$ for this example,

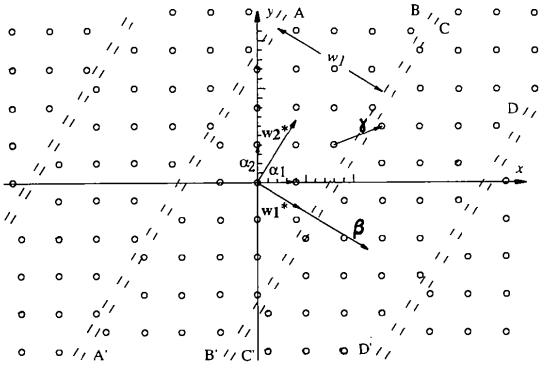

Fig. 1. Schematic diagram of a perfect lattice interrupted by planar faults distributed as a shift lattice. Each lattice point is shown as a circle. Each 'slab' of perfect lattice is of width w_1 and the slabs are a vector distance $\boldsymbol{\beta}$ apart. This particular lattice is square and its parameters are $\mathbf{a}_1 = 4\mathbf{i}$ and $\mathbf{a}_2 = 4\mathbf{j}$ arbitrary units. The lattice in the slab to the right of the central one is displaced one and two units in the x and y directions, respectively, with respect to that in the central slab, *i.e.* $\varepsilon_1 = \frac{1}{4}$ and $\varepsilon_2 = \frac{1}{2}$.

while ε_2 – the corresponding fraction of $\boldsymbol{a}_2$ – is $\frac{1}{2}$. If any integer were added either to ε_1 or ε_2, there would be no difference in the $\delta_{\boldsymbol{a}_1,\boldsymbol{a}_2}$ term in (2.2), since a comb displaced an integral number of lattice parameters which remains invariant. Hence, we may choose the proper fractional form of the εs. In three dimensions, a term $\varepsilon_3\boldsymbol{a}_3$ must be added to the right-hand side of (2.3).

We now state, with the aid of (2.2) and (2.3), the final form of the structure $f(\mathbf{r})$ as

$$f(\mathbf{r}) = \sum_m g[\mathbf{w}_1^* \cdot (\mathbf{r} - m\boldsymbol{\beta})]\, \delta_{\boldsymbol{a}_1,\boldsymbol{a}_2}[\mathbf{r} - m(\varepsilon_1\boldsymbol{a}_1 + \varepsilon_2\boldsymbol{a}_2)]. \tag{2.4}$$

The set of delta functions in (2.4) is merely the skeleton of the structure. Associated with each delta function in any actual material of interest is a motif consisting of an atom or a certain arrangement of atoms. We presume that the approximation is good enough that all motifs in any given structure are identical, so that the material can be represented by the convolution of $f(\mathbf{r})$ in (2.4) with a function representing the motif. If this latter function is, say, $q(\mathbf{r})$, then the material is represented by

$$f(\mathbf{r}) * q(\mathbf{r}) \tag{2.5}$$

where the asterisk denotes convolution.

2.3. *The Fourier transform of the structures*

Since diffraction patterns of materials are (to varying degrees of approximation depending on the nature of the irradiation upon the material) Fraunhofer diffraction patterns, which in turn are the intensity patterns from the Fourier transform of the structure, we need to determine this transform. We define the transform $H(\mathbf{s})$ of $h(\mathbf{r})$ thus:

$$H(\mathbf{s}) = \int h(\mathbf{r}) \exp(-2\pi i\mathbf{r} \cdot \mathbf{s})\mathrm{d}\mathbf{r},$$

where $\mathbf{s}$ is the space reciprocal to $\mathbf{r}$, $\mathrm{d}\mathbf{r}$ is an elementary area in $\mathbf{r}$ space and the integral is over all $\mathbf{r}$. The convention is that a function in $\mathbf{r}$ space is represented by a small letter (here h), while its transform in $\mathbf{s}$ space is represented by the same capital letter (here H).

The *convolution theorem* states that the transform of a convolution of two functions is the product of the individual transforms. Hence the transform of (2.5) is

$$F(\mathbf{s})Q(\mathbf{s}). \tag{2.6}$$

Expressions (2.5) and (2.6) illustrate the central importance of knowing $F(\mathbf{s})$ as a means of obtaining information concerning $f(r)$ from diffraction patterns. It is shown in §5 that

$$F(\mathbf{s}) = A\sum_h \sum_k G(\mathbf{w}_1 \cdot \mathbf{s}_{hk})\, \delta_{\boldsymbol{\beta}*}[\mathbf{s}_{hk} + (h\varepsilon_1 + k\varepsilon_2)\boldsymbol{\beta}^*], \tag{2.7}$$

where

$$\mathbf{s}_{hk} = s - (h\boldsymbol{a}_1^* + k\boldsymbol{a}_2^*), \tag{2.8}$$

A is a positive constant, G is the one-dimensional transform of g (so that if g is a *rect* function, G will be a *sinc* function) and the $\delta_{\boldsymbol{\beta}*}$ term is a comb consisting of a single row of point delta functions spaced $\boldsymbol{\beta}^*$ apart.

Fig. 2 is a schematic diagram of the transform of the structure illustrated in Fig. 1. The solid circles represent point-delta functions of various amplitudes and the open circles the points $h\boldsymbol{a}_1^* + k\boldsymbol{a}_2^*$, *i.e.* the points of the reciprocal lattice whose parameters are $\boldsymbol{a}_1^*$ and $\boldsymbol{a}_2^*$. At these points in $\mathbf{s}$ space, $\mathbf{s}_{hk} = 0$ by (2.8) and so we may take these points as origins in $\mathbf{s}_{hk}$ space for any particular h and k. When $h = k = 0$, the appropriate term $F_{00}(\mathbf{s})$ in (2.7) is

$$F_{00}(\mathbf{s}) = AG(\mathbf{w}_1 \cdot \mathbf{s})\, \delta_{\boldsymbol{\beta}*}(\mathbf{s}),$$

and so, on the slanting line through the origin of u and v in Fig. 2, we see the point-delta functions of the comb $\delta_{\boldsymbol{\beta}*}(\mathbf{s})$, spaced $\boldsymbol{\beta}^*$ apart, amplitude modulated by $G(\mathbf{w}_1 \cdot \mathbf{s})$, the *sinc* function which is the one-dimensional transform of the *rect* function $g(\mathbf{w}_1^* \cdot \mathbf{r})$. The term $F_{10}(\mathbf{s})$ in (2.7), when $h = 1$ and $k = 0$, is $F_{10}(\mathbf{s}) = AG(\mathbf{w}_1 \cdot \mathbf{s}_{10})\, \delta_{\boldsymbol{\beta}*}[\mathbf{s}_{10} + (\boldsymbol{\beta}^*/4)]$ (it being remembered that $\varepsilon_1 = \frac{1}{4}$ in this example) and so we see the reflections, modulated by the same G function as for $h = k = 0$, shifted to the 'north west' by $\boldsymbol{\beta}^*/4$ compared with the unshifted ones astride the origin. We may proceed likewise to interpret the reflections on the slanting line appropriate to any h and k.

3. Applications

3.1. *Crystallographic shear: the* TiO_{2-x} *system*

Structures analogous to that shown in Fig. 1 occur in the crystallographic shear (CS) phases (Hyde &

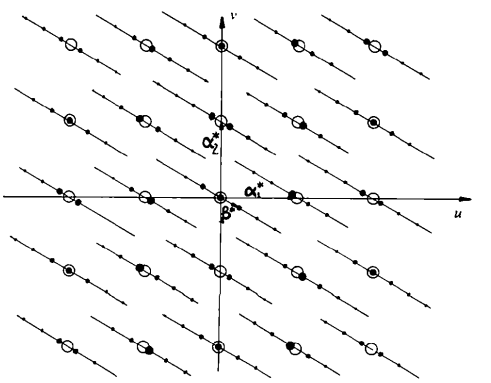

Fig. 2. Schematic diagram of the Fourier transform of the structure in Fig. 1. The reciprocal space $\mathbf{s}$ has Cartesian components u and v. Each slanting line contains the reflections appropriate to one term of (2.7). The open cirlces are the points $h\boldsymbol{a}_1^* + k\boldsymbol{a}_2^*$, so that at these points in s space, $\mathbf{s}_{hk} = 0$ by (2.8). We can therefore imagine the open circles as 'origins' in $\mathbf{s}_{hk}$ space for the reflections appropriate to a particular value of h and k. It is seen that each series of reflections, spaced $\boldsymbol{\beta}^*$ apart, is displaced by $-(h\varepsilon_1 + K\varepsilon_2)\boldsymbol{\beta}^*$, in this case, $-(h/4 + k/2)\boldsymbol{\beta}^*$.

Andersson, 1989; Tilley, 1987). The boundaries of the slabs of perfect parent structure are CS planes which are effectively planes of collapse in which a sheet of O atoms is eliminated from the structure. The CS operation therefore moves the composition of the crystal towards the metal-rich region of the phase diagram. The process will be illustrated here with reference to the reduced rutile system. Initial reduction occurs by collapse on {132} (it being understood throughout this paper that the indices refer to the parent rutile structure), while reduction below a composition of *ca* $TiO_{1.89}$ is accommodated on {121} planes. In the composition range between *ca* $TiO_{1.93}$ and $TiO_{1.89}$, the CS planes swing in orientation from {132} to {121} so that a continuum of orientations is possible. Despite the range of CS planes involved, all have the same collapse vector, $(\frac{1}{2})\langle 011\rangle$. Idealized representations of some of these are shown in Fig. 3. The {132} and swinging CS regions consist of ordered intergrowths of pure CS components as in the {121} CS planes, labelled *C*, and antiphase components as in the {011} planes, labelled *A*.

The relation between the CS parameters and the shift-lattice parameters are simply that $\boldsymbol{\alpha}_1$, $\boldsymbol{\alpha}_2$ and $\boldsymbol{\alpha}_3$ correspond to **a**, **b** and **c**, respectively, and the collapse vector $(\frac{1}{2})\langle 011\rangle$ to $\varepsilon_1 = 0$, $\varepsilon_2 = \varepsilon_3 = \frac{1}{2}$. That the CS planes lie at an angle to the section in Fig. 3 is a reflection of the fact that the vector β is not in this plane.

We now make a point concerning the nature of the motif function $q(\mathbf{r})$ introduced earlier. An examination of Fig. 3 shows that it is the Ti atoms that are distributed as a shift lattice, while the O atoms form merely a crystallographic framework. It should be emphasized, therefore, that the structures shown, taken in their entirety, are not shift-lattice distributed, but merely that the Ti atoms in it are so distributed. The function $q(\mathbf{r})$ therefore represents the scattering factor of one Ti atom in this example.

The form of the diffraction patterns generated by such structures is shown by Hyde & Andersson (1989) (Fig. 48, p. 102). The diffraction patterns conform in appearance to that shown in Fig. 2. In some cases, the line of spots from the origin, in a $\boldsymbol{\beta}^*$ direction, points towards a main reflection. In any one line of such spots, those immediately surrounding different main reflections may be incommensurate with each other, depending upon $|\boldsymbol{\beta}^*|$. We have, therefore, in the swinging region, two levels of incommensurability. If the direction of $\boldsymbol{\beta}^*$ is such that it fails to point from the origin towards any main reflection, then the structure is automatically incommensurate. If, on the other hand, $\boldsymbol{\beta}^*$ does point to a main reflection, as in the case of ordered arrays of the planar boundaries shown in Fig. 3, then the boundaries of the *g* functions are still in the direction of a crystallographic plane, but the structure will be incommensurate if $|\boldsymbol{\beta}^*|$ is such that the phase of each succeeding *g* function boundary is changing with respect to the underlying crystal structure.

3.2. *Antiphase boundaries: the* Au–Mn *system*

The Au–Mn system of alloys contains a number of complex structures. These are basically derived from a cubic parent structure broken up by a variety of different antiphase boundaries (van Tendeloo & Amelinckx, 1979; van Tendeloo, Wolf, van Dyke & Amelinckx, 1978). Of interest here are the two compounds Au_3Mn and Au_5Mn_2. The structure of Au_3Mn is shown in Fig. 4(*a*). It consists of alternating sheets of Au and Mn atoms. The structure of the Au_5Mn_2 phase is, in effect, a CS structure which may be geometrically derived from the parent by the removal of every sixth Au plane and subsequent collapse of the structure. The result of this operation is shown in Fig. 4(*b*). The relationship between these crystallographic parameters and the shift-lattice parameters can be seen from Fig. 4 to be $\boldsymbol{\alpha}_1 = \mathbf{c}$, $\boldsymbol{\alpha}_2 = \mathbf{a}$, $\boldsymbol{\alpha}_3$ being, in shift-lattice terms, redundant. Similarly, the shift parameters are $\varepsilon_1 = \frac{1}{4}$, $\varepsilon_2 = \frac{1}{2}$ with ε_3 not being needed.

The diffraction pattern from this space, which is shown in Fig. 4(*c*), does not, at first sight, conform to that illustrated in Fig. 2. This is due to the fact that the planar boundaries in the Au-deficient structure are rather close together and the 'superlattice' spots are commensurate. If the planar boundaries are imagined to move further apart, it is possibe to visualize, by reference to Fig. 2, that the 'superlattice' reflections will approach each other, and that the envelope of these groups of spots will become narrower, leading to diffraction patterns closely resembling those shown in Fig. 2.

3.3. *New structures*

By varying the shift-lattice parameters even slightly, one can construct many motif arrangements and estimate the form of their diffraction patterns without recourse to traditional diffraction theory. This has a great advantage when long-period or incommensurate phases are involved. Indeed, it is a straightforward procedure to construct large numbers of new hypothetical structures from experimentally observed shift-lattice parameters, as can be illustrated with respect to the TiO_2-related structures. This system has been selected because, despite the considerable amount of work which has already been published on these structures, new possibilities are easily generated.

As outlined above, in the rutile-based CS structures, the CS planes run from (121) to (132) and consist of regularly ordered sequences of the antiphase boundary element *A* and the collapse element *C*, which alternate along the length of the CS plane. The *C* and *A* components are separated as much as possible along the CS plane length, leading to the 'principle of maximum dispersion' suggested by Hyde & Andersson (1989). All these structures can be generated by a variation of the argument of *g*. However, ambiguities can occur, as pointed out by Hyde & Andersson (1989), and

these can similarly be produced and are shown for the case of {132} CS in Figs. 5(*a*), (*b*) and (*c*). In Figs. 5(*a*) and (*b*) (in which the bounds of the *g* functions which give rise to the structures are shown as continuous lines), both of the CS planes shown consist of alternating *AC* sequences. The composition of the two structures will be be the same. The unit cells will be different, however, and in practice, which of the two structures actually

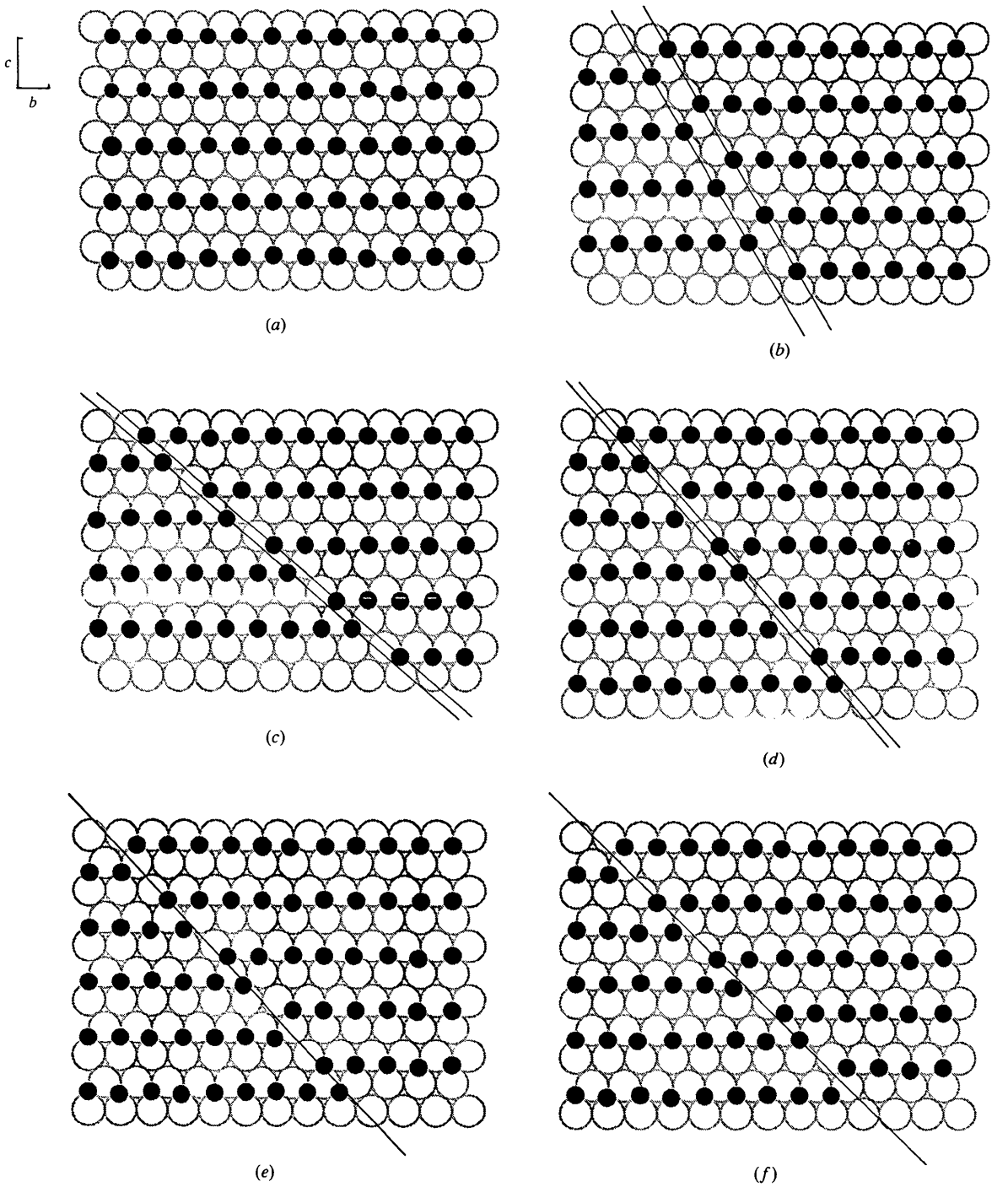

Fig. 3. Idealized representation of planar boundaries found in reduced rutile: (*a*) the rutile structure; (*b*) an antiphase boundary on (011), made up entirely of *A* units; (*c*) trace of CS plane (121), ...*CCC*...; (*d*) CS plane (132), ...*ACAC*...; (*e*) CS pane (253), ...*ACCACC*...; (*f*) CS plane (374), ...*ACCC*.... The open circles represent O atoms and the filled circles Ti atoms.

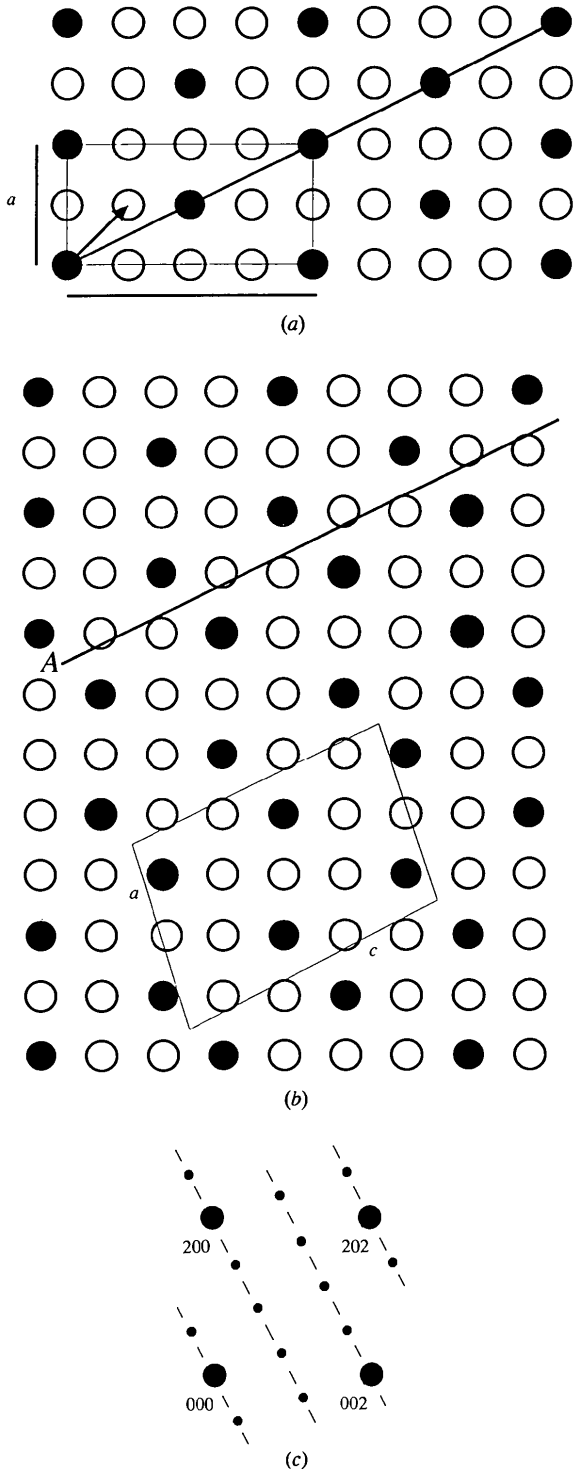

Fig. 4. (*a*) The Au_3Mn structure. The open circles represent Au and the filled circles Mn. The diagonal line through the Mn atoms shows a collapse plane. Collapse by the vector indicated at the lower left eliminates a plane of Au atoms. Regular repetition of this operation leads to the Au_5Mn_2 structure shown in (*b*). (*c*) Schematic diagram of the $h0l_{f.c.c.}$ plane of the diffraction pattern from Au_5Mn_2, from van Tendeloo, Woolf, van Dyke & Amelinckx (1978).

forms may depend upon terms such as strain energy introduced by metal–metal interactions in the boundaries. In Fig. 5(*c*), the sequence of units down each plane is the same and the planes are alternately *A* and *C* types. The composition of the crystal remains the same as in the first two cases, however, as the total number of *A* units

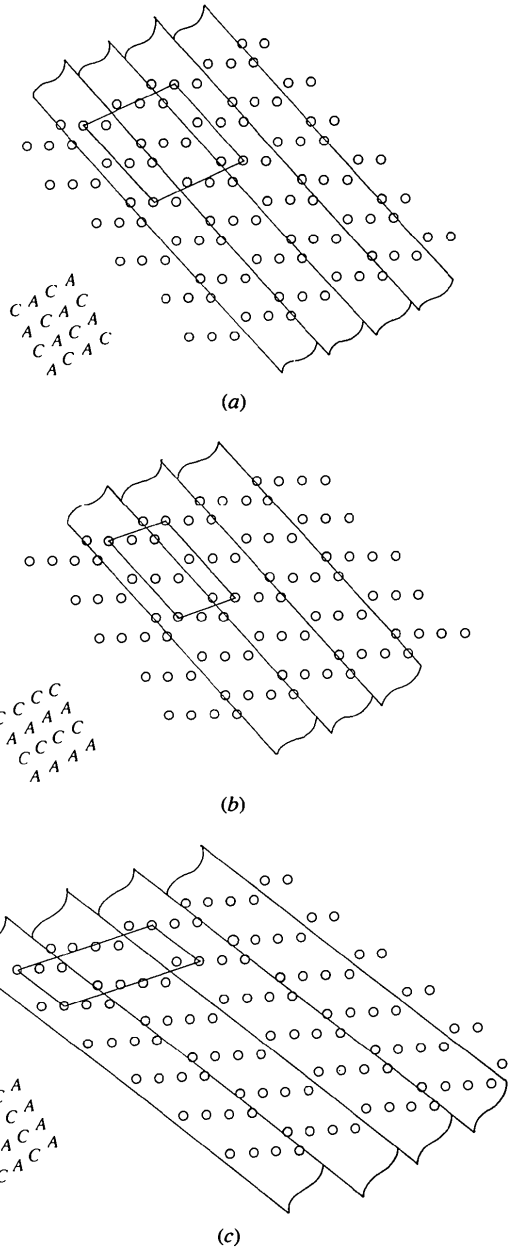

Fig. 5. (*a*)–(*c*) Schematic diagrams of 132 boundaries in rutile, with only metal-atom positions shown. The *g* functions are shown as lines. Three different patterns result, all of which have the same composition. The heavy lines outline the simplest unit cells. The patterns of the collapsed (*C*) and antiphase (*A*) structure in each case are summarized to the left of every diagram.

remains the same as that of C units. The change in arrangement is brought about by varying the width of the g functions slightly with respect to those in the first two diagrams. In the pair of diagrams Figs. 6(a) and (b), two arrangements are shown for (253) CS. Although the same ambiguities just illustrated for the (132) case can also be drawn for this structure, we choose instead to display a composition anomaly. The CS planes normally observed are depicted in Fig. 6(a) and consist of repeating sequences CCA. The alternative arrangement AAC shown in Fig. 6(b) is oxygen-rich compared with that in Fig. 6(a). Finally, we note with respect to Figs. 5 and 6 that many other arrangements of the A and C motifs can be depicted and by systematically widening the g-function envelopes, without changing their orientation or degree of overlap, we may create a homologous series of structures for each arrangement.

The widths of the unit cells of the structures depicted in Figs. 5(a) and (c) are twice the spacing β of the g functions, while in the remaining portions of Fig. 5 and 6 they are equal to $\boldsymbol{\beta}$. For other choices of $\boldsymbol{\beta}$, the width of the unit cell may be any integral multiple of $\boldsymbol{\beta}$ or, in the case of a truly incommensurate structure, infinity. With the shift-lattice view of these structures, however, the unit-cell size assumes a position of lesser importance; the fundamental quantity determining the positions of the diffraction spots is the inter-g-function spacing $\boldsymbol{\beta}$, as is made clear in (2.7) by the existence of the $\delta_{\beta *}$ comb.

As an example of the rich variety of structures which may be generated by the shift-lattice principle, we show, in Fig. 7, a shift lattice (based on the same subcell as that in Figs. 5 and 6) with overlapping g functions. The nature of the boundaries is here more complex than in the previous two figures, giving the motif pattern the appearance of arrays consisting of hexagons of two different sizes.

The diffraction patterns from these constructions may be derived by application of the rules described earlier. The theory presented in this paper allows one quickly to see the essential features of the diffraction patterns of a wide variety of lattices with planar faults without the necessity of performing a Fourier transform on a particular structure. In other words, it enables a specimen to be surveyed in reciprocal space as a member of a genus rather than in isolation.

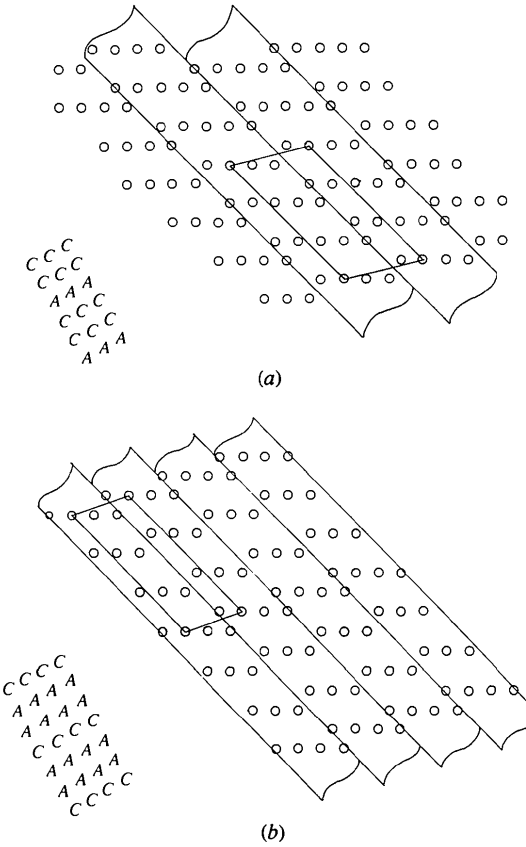

Fig. 6. (a) and (b) Schematic diagrams of 253 boundaries in rutile, with only the metal-atom positions shown. The g functions are shown as lines. The convention adopted is that a motif falling exactly on a line is included. The two patterns which are depicted represent different compositions, although the boundaries have the same indices.

4. Concluding remarks

In this paper, crystals made up of ordered repeating slices of a parent structure have been explored as examples of shift lattices and the general form of the appropriate Fourier transforms of these structures has been

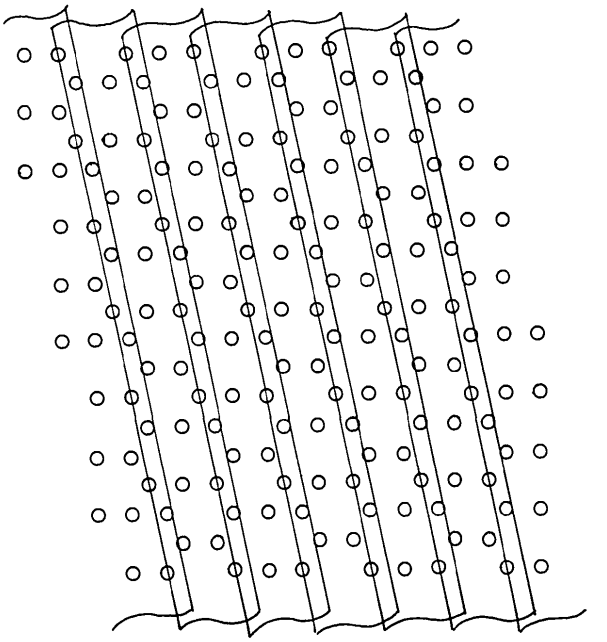

Fig. 7. A hypothetical structure based on the same sublattice and having the same ε_1 and ε_2 as those of Figs. 5 and 6. Here, the g functions overlap and a pattern of radically different character is produced.

developed. Unlike earlier papers (Harburn, Tilley, Williams & Williams, 1991, 1993), which dealt with one-dimensional cases, the theory in this paper covers all possible planar shift-lattice distributed slabs of perfect crystals with an arbitrary three-dimensional vector shift between neighbouring slabs. In this way, antiphase boundaries, CS structures and many other configurations may be treated and their diffraction patterns visualized. In addition, it is noted that the theory does not need the lattice fragments which are in shift-lattice relationships with one another to be in physical contact. Hence, the structures built up of two or more lattice fragments can be formed as well as the diffraction patterns that they give rise to, provided that the shift-lattice rules are obeyed. Such an approach has been used to interpret the structures of some L-Ta_2O_5-related oxides (Harburn, Tilley, Williams & Williams, 1993).

It is gradually becoming evident that a large variety of different solids have shift-lattice formations of one sort or another. The overview provided by the shift-lattice approach to structures built up from ordered arrays of planar faults and the diffraction patterns which they give rise to, which has been given here, allows broad families of apparently different structure types to be related one to another and new structures to be suggested. This procedure has a utility in aiding the search for new structures and suggesting interpretations of incommensurate diffraction patterns. In addition, it poses a question for the crystal chemist, who has to explain why one arrangement is preferred to another.

Appendix

Introduction

Although some of the results presented earlier in this paper are three-dimensional, the analysis presented here will, for the sake of brevity, be two-dimensional, there being no formal difficulty in the extension to three dimensions, but merely more symbols. We now list the various standard results which we shall need in the analysis; they are all to be found in, or easily derived from, results in the books by Bracewell (1978) or Champeney (1973, 1987).

With $\mathbf{r}$ as the position vector in the plane, we may define the point-delta function with its singularity at the origin, namely $\delta(\mathbf{r})$, by the equation

$$\int \delta(\mathbf{r})\,\varphi(\mathbf{r})\,d\mathbf{r} = \varphi(\mathbf{O}), \tag{A1}$$

where $d\mathbf{r}$ is an elementary area in $\mathbf{r}$ space. This equation is to be interpreted as follows. If (A1) is true for *any* function $\varphi(\mathbf{r})$, which is finite and continuous in the neighbourhood of the origin, then the symbol $\delta(\mathbf{r})$ in that equation describes the required point-delta function. It may be visualized as a 'spike' of infinite height and zero width at the origin of $\mathbf{r}$ such that is integrated volume is unity.

The idea of the *comb* is central to this analysis and we state here the useful notation

$$\delta_a(x) = \sum_m \delta(x - ma) \tag{A2}$$

due to Hsu (1967). We next state the identity

$$\delta_1(x) = \sum_m \exp(-2\pi imx) \tag{A3}$$

which is treated in standard books on Fourier-transform theory and discussed in some detail by Harburn, Tilley, Williams & Williams (1993).

Extending this notation to two dimensions, we may define two types of comb, namely the point comb

$$\delta_{\mathbf{a}}(\mathbf{r}) = \sum_m \delta(\mathbf{r} - m\mathbf{a}) \tag{A4}$$

and the two-dimensional comb

$$\delta_{\mathbf{a}_1,\mathbf{a}_2}(\mathbf{r}) = \sum_m \sum_n \delta[\mathbf{r} - (m\mathbf{a}_1 + n\mathbf{a}_2)]. \tag{A5}$$

Equation (A4) describes a single row of point singularities spaced $\mathbf{a}$ apart in $\mathbf{r}$ space, while (A5) describes a two-dimensional lattice with parameters $\mathbf{a}_1$ and $\mathbf{a}_2$.

We next mention the well known concept of reciprocal vectors, namely that a set $\mathbf{a}_1^*$, $\mathbf{a}_2^*$ of vectors *reciprocal* to the set $\mathbf{a}_1$, $\mathbf{a}_2$ (these latter two vectors being non-zero and not parallel or antiparallel to each other) may be defined by the equation

$$\begin{pmatrix} \mathbf{a}_1^* \cdot \mathbf{a}_1 & \mathbf{a}_1^* \cdot \mathbf{a}_2 \\ \mathbf{a}_2^* \cdot \mathbf{a}_1 & \mathbf{a}_2^* \cdot \mathbf{a}_2 \end{pmatrix} = I, \tag{A6}$$

where I is the unit matrix. A fundamental property of reciprocal vectors is their appearance in the expansion of an arbitrary vector in terms of any two basis vectors, say $\mathbf{a}_1$ and $\mathbf{a}_2$. Specifically, any vectror $\mathbf{r}$ may be expressed as

$$\mathbf{r} = (\mathbf{a}_1^* \cdot \mathbf{r})\mathbf{a}_1 + (\mathbf{a}_2^* \cdot \mathbf{r})\mathbf{a}_2, \tag{A7}$$

as may readily be shown from (A6). We may also state, using reciprocal vectors, a two-dimensional version of the Fourier-transform similarity theorem, namely that if

$$\mathcal{F}f(x, y) = F(u, v)$$

($\mathbf{r}$ having rectangular Cartesian components x and y and the reciprocal space $\mathbf{s}$ having the corresponding components u and v), then

$$\mathcal{F}f(\mathbf{a}_1^* \cdot \mathbf{r}, \mathbf{a}_2^* \cdot \mathbf{r}) = |A_{\mathbf{a}_1,\mathbf{a}_2}| F(\mathbf{a}_1 \cdot \mathbf{s}, \mathbf{a}_2 \cdot \mathbf{s}),$$

where $A_{\mathbf{a}_1,\mathbf{a}_2}$ is the area of the parallelogram defined by the vectors $\mathbf{a}_1$ and $\mathbf{a}_2$. We shall, in fact, need only a special case of the above equation, namely that if

$$\mathcal{F}f_1(x)f_2(y) = F_1(u)F_2(v)$$

(F_1 and F_2 being the one-dimensional transforms of f_1

and f_2, respectively), then

$$\mathcal{F}f_1(\mathbf{a}_1^* \cdot \mathbf{r})f_2(\mathbf{a}_2^* \cdot \mathbf{r}) = |A_{\mathbf{a}_1,\mathbf{a}_2}|\, F_1(\mathbf{a}_1 \cdot \mathbf{s})\, F_2(\mathbf{a}_2 \cdot \mathbf{s}). \quad \text{(A8)}$$

The above generalization of the similarity theorem may be derived in reciprocal-vector form from the matrix form treated by, for example, Jones (1982) and Arsac (1966).

We now state the shift theorem, namely that if $\mathcal{F}f(\mathbf{r}) = F(\mathbf{s})$, then

$$\mathcal{F}f(\mathbf{r} - \mathbf{r}_O) = \exp(-2\pi i \mathbf{r}_O \cdot \mathbf{s})F(\mathbf{s}), \quad \text{(A9)}$$

where $\mathbf{r}_O$ is a constant vector in $\mathbf{r}$ space.

Two-dimensional convolution of two functions f_1 and f_2 is defined as

$$f_1(\mathbf{r}) * f_2(\mathbf{r}) = \int f_1(\mathbf{t})f_2(\mathbf{r} - \mathbf{t})\,\mathrm{d}\mathbf{t}, \quad \text{(A10)}$$

where $\mathbf{t}$ is a dummy variable in $\mathbf{r}$ space and the integral is over all $\mathbf{t}$. The version of the convolution theorem that we shall need is

$$\mathcal{F}f_1(\mathbf{r})f_2(\mathbf{r}) = F_1(\mathbf{s}) * F_2(\mathbf{s}). \quad \text{(A11)}$$

We shall also need the identity

$$\delta(\mathbf{s}) = |A_{\mathbf{a}_1,\mathbf{a}_2}|\delta(\mathbf{a}_1 \cdot \mathbf{s})\,\delta(\mathbf{a}_2 \cdot \mathbf{s}). \quad \text{(A12)}$$

Equation (A12) may be interpreted as follows. The delta function $\delta(\mathbf{a}_1 \cdot \mathbf{s})$ in two dimensions is a line-delta function whose singularity is a straight line through the origin of $\mathbf{r}$ space perpendicular to the vector $\mathbf{a}_1$. Similarly, $\delta(\mathbf{a}_2 \cdot \mathbf{s})$ has its singularity on a line perpendicular to $\mathbf{a}_2$. The point of intersection of the lines $\mathbf{a}_1 \cdot \mathbf{s} = 0$ and $\mathbf{a}_2 \cdot \mathbf{s} = 0$ (namely the origin) is the position of the point singularity of $\delta(\mathbf{s})$. The term $|A_{\mathbf{a}_1,\mathbf{a}_2}|$ may be derived by putting both sides of (A12) in turn into the definition (A1) of the delta function.

Finally, we state that the Fourier transform of a two-dimensional comb is another comb; specifically

$$\mathcal{F}\,\delta_{\mathbf{a}_1,\mathbf{a}_2}(\mathbf{r}) = |A_{\mathbf{a}_1^*,\mathbf{a}_2^*}|\,\delta_{\mathbf{a}_1^*,\mathbf{a}_2^*}(\mathbf{s}), \quad \text{(A13)}$$

a result standard to crystallography, which is discussed in many textbooks on the subject, for example, Woolfson (1970).

The Fourier transform of the representation of a shift-lattice distributed system of planar faults in an otherwise perfect crystal lattice

It is explained in some detail in §2 that the two-dimensional structure $f(\mathbf{r})$, with which we are concerned in this paper, may be represented by

$$f(\mathbf{r}) = \sum_m g[\mathbf{w}_1^* \cdot (\mathbf{r} - m\boldsymbol{\beta})]\,\delta_{\boldsymbol{\alpha}_1,\boldsymbol{\alpha}_2}(\mathbf{r} - m\boldsymbol{\gamma}), \quad \text{(A14)}$$

where $\boldsymbol{\gamma}$ is the vector describing the displacement between the perfect crystal lattice inscribed in one slab and that inscribed in a neighbouring slab. It is our purpose here to obtain a suitable expression for the transform of (A14). We begin by transforming this equation term by term using the convolution theorem (A11), the similarity theorem (A8) (with $\mathbf{w}_1^*$ and $\mathbf{w}_2^*$ as a set of vectors to which $\mathbf{w}_1$ and $\mathbf{w}_2$ are reciprocal), the shift theorem (A9) and the transform (A13) of the two-dimensional comb. We obtain

$$F(\mathbf{s}) = \sum_m [|A_{\mathbf{w}_1,\mathbf{w}_2}|G(\mathbf{w}_1 \cdot \mathbf{s})\,\delta(\mathbf{w}_2 \cdot \mathbf{s})\exp(-2\pi i m\boldsymbol{\beta} \cdot \mathbf{s})] * [|A_{\boldsymbol{\alpha}_1^*,\boldsymbol{\alpha}_2^*}|\,\delta_{\boldsymbol{\alpha}_1^*,\boldsymbol{\alpha}_2^*}(\mathbf{s})\exp(-2\pi i m\boldsymbol{\gamma} \cdot \mathbf{s})]. \quad \text{(A15)}$$

Here G is, of course, the one-dimensional transform of g defined by

$$G(u) = \int g(x)\exp(-2\pi i u x)\,\mathrm{d}x.$$

We now expand (A15) by the definition (A10) of convolution and obtain

$$F(\mathbf{s}) = A' \sum_m \int \delta_{\boldsymbol{\alpha}_1^*,\boldsymbol{\alpha}_2^*}(\mathbf{t})\exp(-2\pi i m\boldsymbol{\gamma} \cdot \mathbf{t})\,G[\mathbf{w}_1 \cdot (\mathbf{s} - \mathbf{t})] \times \delta[\mathbf{w}_2 \cdot (\mathbf{s} - \mathbf{t})]\exp[-2\pi i m\boldsymbol{\beta} \cdot (\mathbf{s} - \mathbf{t})]\,\mathrm{d}\mathbf{t}, \quad \text{(A16)}$$

where $A' = |A_{\mathbf{w}_1,\mathbf{w}_2}A_{\boldsymbol{\alpha}_1^*,\boldsymbol{\alpha}_2^*}|$. We rearrange (A16) thus

$$F(\mathbf{s}) = A' \int \delta_{\boldsymbol{\alpha}_1^*,\boldsymbol{\alpha}_2^*}(\mathbf{t})\,G[\mathbf{w}_1 \cdot (\mathbf{s} - \mathbf{t})]\,\delta[\mathbf{w}_2 \cdot (\mathbf{s} - \mathbf{t})] \times \sum_m \exp\{-2\pi i m[(\boldsymbol{\gamma} - \boldsymbol{\beta}) \cdot \mathbf{t} + \boldsymbol{\beta} \cdot \mathbf{s}]\}\,\mathrm{d}\mathbf{t}.$$

Applying the identity (A3) to the sum of exponentials, we obtain

$$F(\mathbf{s}) = A' \int \delta_{\boldsymbol{\alpha}_1^*,\boldsymbol{\alpha}_2^*}(\mathbf{t})\,G[\mathbf{w}_1 \cdot (\mathbf{s} - \mathbf{t})] \times \delta[\mathbf{w}_2 \cdot (\mathbf{s} - \mathbf{t})]\,\delta_1[(\boldsymbol{\gamma} - \boldsymbol{\beta}) \cdot \mathbf{t} + \boldsymbol{\beta} \cdot \mathbf{s}]\,\mathrm{d}\mathbf{t}.$$

We now expand $\delta_{\boldsymbol{\alpha}_1^*,\boldsymbol{\alpha}_2^*}(\mathbf{t})$ by means of (A5); it is convenient to use

$$h\boldsymbol{\alpha}_1^* + k\boldsymbol{\alpha}_2^* = \boldsymbol{\alpha}_{hk}^*,$$

where h and k are integers. We obtain

$$\begin{aligned} F(\mathbf{s}) &= A' \sum_h \sum_k \int \delta(\mathbf{t} - \boldsymbol{\alpha}_{hk}^*)\,G[\mathbf{w}_1 \cdot (\mathbf{s} - \mathbf{t})] \times \delta[\mathbf{w}_2 \cdot (\mathbf{s} - \mathbf{t})]\,\delta_1[(\boldsymbol{\gamma} - \boldsymbol{\beta}) \cdot \mathbf{t} + \boldsymbol{\beta} \cdot \mathbf{s}]\,\mathrm{d}\mathbf{t} \\ &= A' \sum_h \sum_k G[\mathbf{w}_1 \cdot (\mathbf{s} - \boldsymbol{\alpha}_{hk}^*)] \times \delta[\mathbf{w}_2 \cdot (\mathbf{s} - \boldsymbol{\alpha}_{hk}^*)]\,\delta_1[(\boldsymbol{\gamma} - \boldsymbol{\beta}) \cdot \boldsymbol{\alpha}_{hk}^* + \boldsymbol{\beta} \cdot \mathbf{s}] \end{aligned}$$

by (A1). With $\mathbf{s} - \boldsymbol{\alpha}_{hk}^* = \mathbf{s}_{hk}$, this becomes

$$F(\mathbf{s}) = A' \sum_h \sum_k G(\mathbf{w}_1 \cdot \mathbf{s}_{hk})\,\delta(\mathbf{w}_2 \cdot \mathbf{s}_{hk})\,\delta_1(\boldsymbol{\beta} \cdot \mathbf{s}_{hk} + \boldsymbol{\gamma} \cdot \boldsymbol{\alpha}_{hk}^*). \quad \text{(A17)}$$

The product of the δ function and the δ_1 function in each term of (A17) is a comb consisting of a single row of equispaced point singularities; our remaining task is to get it into the form of (A4) which will reveal exactly where each 'tooth' of the comb resides in s space. We

use

$$T = \delta(\mathbf{w}_2 \cdot \mathbf{s}_{hk})\,\delta_1(\boldsymbol{\beta} \cdot \mathbf{s}_{hk} + \boldsymbol{\gamma} \cdot \boldsymbol{\alpha}^*_{hk})$$
$$= \sum_p \delta(\mathbf{w}_2 \cdot \mathbf{s}_{hk})\,\delta(\boldsymbol{\beta} \cdot \mathbf{s}_{hk} + \boldsymbol{\gamma} \cdot \boldsymbol{\alpha}^*_{hk} - p)$$

by (A2). We now use $K_p = p - \boldsymbol{\gamma} \cdot \boldsymbol{\alpha}^*_{hk}$, whereupon

$$T = \sum_p \delta(\mathbf{w}_2 \cdot \mathbf{s}_{hk})\,\delta[\boldsymbol{\beta} \cdot (\mathbf{s}_{hk} - k_p\boldsymbol{\beta}^*)], \qquad \text{(A18)}$$

where $\boldsymbol{\beta}, \mathbf{w}_2$ are the vectors reciprocal to $\boldsymbol{\beta}^*, \mathbf{w}^*_2$. (Although we are using $\mathbf{w}_2$ as a vector in two reciprocal systems, namely that reciprocal to $\mathbf{w}^*_1, \mathbf{w}^*_2$ and also $\mathbf{w}^*_2, \boldsymbol{\beta}^*$, the vectors $\boldsymbol{\beta}^*$ and $\mathbf{w}^*_2$ are unique since both systems are orthogonal. Were they not so, we would have to define two *different* vectors $\mathbf{w}_2$ in the two different systems.) In order to equate (A18) with a comb of the form (A4), we need to express (A18) in the form

$$T = \sum_p \delta[\mathbf{w}_2 \cdot (\mathbf{s}_{hk} - \mathbf{S})]\,\delta[\boldsymbol{\beta} \cdot (\mathbf{s}_{hk} - \mathbf{S})], \qquad \text{(A19)}$$

where $\mathbf{S}$ is a vector to be determined To do this, we proceed as follows. First, we compare (A18) and (A19), whence

$$\mathbf{w}_2 \cdot \mathbf{S} = 0 \text{ and } \boldsymbol{\beta} \cdot \mathbf{S} = \boldsymbol{\beta} \cdot k_p\boldsymbol{\beta}^* = K_p \qquad \text{(A20)}$$

by (A6). We now expand $\mathbf{S}$ as a linear combination of the set $\mathbf{w}^*_2, \boldsymbol{\beta}^*$ (whose reciprocal set is $\mathbf{w}_2, \boldsymbol{\beta}$) using (A7) and obtain

$$\mathbf{S} = (\mathbf{w}_2 \cdot \mathbf{S})\mathbf{w}^*_2 + (\boldsymbol{\beta} \cdot \mathbf{S})\boldsymbol{\beta}^*$$
$$= K_p\boldsymbol{\beta}^*$$

by (A20). Therefore, (A19) becomes

$$T = \sum_p \delta[\mathbf{w}_2 \cdot (\mathbf{s}_{hk} - K_p\boldsymbol{\beta}^*)]\,\delta[\boldsymbol{\beta} \cdot (\mathbf{s}_{hk} - K_p\boldsymbol{\beta}^*)]$$
$$= |A_{\mathbf{w}_2,\boldsymbol{\beta}}| \sum_p \delta(\mathbf{s}_{hk} - K_p\boldsymbol{\beta}^*),$$

by (A12)

$$T = |A_{\mathbf{w}_2,\boldsymbol{\beta}}| \sum_p \delta\{[\mathbf{s}_{hk} + (\boldsymbol{\gamma} \cdot \boldsymbol{\alpha}^*_{hk})\boldsymbol{\beta}^*] - p\boldsymbol{\beta}^*\}$$
$$= |A_{\mathbf{w}_2,\boldsymbol{\beta}}|\,\delta_{\boldsymbol{\beta}^*}[\mathbf{s}_{hk} + (\boldsymbol{\gamma} \cdot \boldsymbol{\alpha}^*_{hk})\boldsymbol{\beta}^*],$$

by (A4). Therefore, (A17) becomes

$$F(\mathbf{s}) = A \sum_h \sum_k G(\mathbf{w}_1 \cdot \mathbf{s}_{hk})\,\delta_{\boldsymbol{\beta}^*}[\mathbf{s}_{hk} + (\boldsymbol{\gamma} \cdot \boldsymbol{\alpha}^*_{hk})\boldsymbol{\beta}^*], \qquad \text{(A21)}$$

where $A = A'|A_{w_2,\boldsymbol{\beta}}|$.

Equation (A21) is a tractable form of the transform of (A14). However, it proved useful in our discussion in §2 to particularize $\boldsymbol{\gamma}$ by putting it into the form

$$\boldsymbol{\gamma} = \varepsilon_1\boldsymbol{\alpha}_1 + \varepsilon_2\boldsymbol{\alpha}_2$$

(where ε_1 and ε_2 may be regarded as the fractions of $\boldsymbol{\alpha}_1$ and $\boldsymbol{\alpha}_2$, respectively, by which the perfect lattice suffers displacement at a planar fault). We have immediately

$$\boldsymbol{\gamma} \cdot \boldsymbol{\alpha}_{hk} = (\varepsilon_1\boldsymbol{\alpha}_1 + \varepsilon_2\boldsymbol{\alpha}_2) \cdot (h\boldsymbol{\alpha}^*_1 + k\boldsymbol{\alpha}^*_2)$$
$$= h\varepsilon_1 + k\varepsilon_2,$$

by (A6). We therefore finally obtain, in two dimensions, the following: if

$$f(\mathbf{r}) = \sum_m g[\mathbf{w}^*_1 \cdot (\mathbf{r} - m\boldsymbol{\beta})]\,\delta_{\boldsymbol{\alpha}_1,\boldsymbol{\alpha}_2}[\mathbf{r} - m(\varepsilon_1\boldsymbol{\alpha}_1 + \varepsilon_2\boldsymbol{\alpha}_2)],$$

then

$$F(\mathbf{s}) = A \sum_h \sum_k G(\mathbf{w}_1 \cdot \mathbf{s}_{hk})\,\delta_{\boldsymbol{\beta}^*}[\mathbf{s}_{hk} + (h\varepsilon_1 + k\varepsilon_2)\boldsymbol{\beta}^*],$$

where $\mathbf{s}_{hk} = \mathbf{s} - \boldsymbol{\alpha}^*_{hk}$ and $\boldsymbol{\alpha}^*_{hk} = h\boldsymbol{\alpha}^*_1 + k\boldsymbol{\alpha}^*_2$.

The analysis in three dimensions proceeds along lines identical to the above and we find that if

$$f(\mathbf{r}) = \sum_m g[\mathbf{w}^*_1 \cdot (\mathbf{r} - m\boldsymbol{\beta})]$$
$$\times\, \delta_{\boldsymbol{\alpha}_1,\boldsymbol{\alpha}_2,\boldsymbol{\alpha}_3}[\mathbf{r} - m(\varepsilon_1\boldsymbol{\alpha}_1 + \varepsilon_2\boldsymbol{\alpha}_2 + \varepsilon_3\boldsymbol{\alpha}_3)],$$

then

$$F(\mathbf{s}) = V \sum_h \sum_k \sum_l G(\mathbf{w}_1 \cdot \mathbf{s}_{hkl})$$
$$\times\, \delta_{\boldsymbol{\beta}^*}[\mathbf{s}_{hkl} + (h\varepsilon_1 + k\varepsilon_2 + l\varepsilon_3)\boldsymbol{\beta}^*],$$

where $\mathbf{s}_{hkl} = \mathbf{s} - (h\boldsymbol{\alpha}^*_1 + k\boldsymbol{\alpha}^*_2 + l\boldsymbol{\alpha}^*_3)$ and V is a combination of volumes analogous to A.

References

ARSAC, J. (1966). *Fourier Transforms and the Theory of Distributions.* New York: Prentice-Hall.

BRACEWELL, R. (1978). *The Fourier Transform and its Applications.* New York: McGraw-Hill.

CHAMPENEY, D. C. (1973). *Fourier Transforms and their Applications.* New York: Academic Press.

CHAMPENEY, D. C. (1987). *A Handbook of Fourier Theorems.* Cambridge Univ. Press.

HARBURN, G., PARRY, B. H., TILLEY, R. J. D. & WILLIAMS, R. P. (1992). *Aust. J. Chem.* **45**, 1397–1413.

HARBURN, G., TILLEY, R. J. D., WILLIAMS, J. M. & WILLIAMS, R. P. (1991). *Nature*, **350**, 214.

HARBURN, G., TILLEY, R. J. D., WILLIAMS, J. M. & WILLIAMS, R. P. (1993). *Proc. R. Soc.* **440**, 23–36.

HSU, H. P. (1967). *Outline of Fourier Analysis.* London: Iliffe Books, Ltd.

HYDE, B. G. & ANDERSSON, S. (1989). *Inorganic Crystal Structures.* New York: Wiley Interscience.

JONES, D. S. (1982). *The Theory of Generalised Functions.* Cambridge Univ. Press.

TENDELOO, G. VAN & AMELINCKX, S. (1979). *Phys. Status Solidus A*, **51**, 141.

TENDELOO, G. VAN, WOLF, R., VAN DYKE, D. & AMELINCKX, S. (1978). *Phys. Status Solidus A*, **47**, 105.

TILLEY, R. J. D. (1987). *Defect Crystal Chemistry*, Ch. 9. Glasgow, London: Blackie.

TILLEY, R. J. D. & WILLIAMS, R. P. (1995). *Philos. Mag.* In the press.

WADSLEY, A. D. (1963). In *Non-stoichiometric Compounds*, edited by L. MANDELCORN, Ch. 3. New York: Academic Press.

WOOLFSON, M. M. (1970). *An Introduction to X-ray Crystallography.* Cambridge Univ. Press.